Molecular Cell *21*, 3–14, January 6, 2006 ©2006 Elsevier Inc. DOI 10.1016/j.molcel.2005.10.035

Coherence and Timing of Cell Cycle Start Examined at Single-Cell Resolution

James M. Bean,[1] Eric D. Siggia,[2] and Frederick R. Cross[1,*]
[1] The Rockefeller University
New York, New York 10021
[2] Center for Studies in Physics and Biology
The Rockefeller University
New York, New York 10021

Summary

Cell cycle "Start" in budding yeast involves induction of a large battery of G1/S-regulated genes, coordinated with bud morphogenesis. It is unknown how intra-Start coherence of these events and inter-Start timing regularity are achieved. We developed quantitative time-lapse fluorescence microscopy on a multicell-cycle timescale, for following expression of unstable GFP under control of the G1 cyclin *CLN2* promoter. Swi4, a major activator of the G1/S regulon, was required for a robustly coherent Start, as *swi4* cells exhibited highly variable loss of cooccurrence of regular levels of *CLN2pr-GFP* expression with budding. In contrast, other known Start regulators Mbp1 and Cln3 are not needed for coherence but ensure regular timing of Start onset. The interval of nuclear retention of Whi5, a Swi4 repressor, largely accounts for wild-type mother-daughter asymmetry and for variable Start timing in *cln3 mbp1* cells. Thus, multiple pathways may independently suppress qualitatively different kinds of noise at Start.

Introduction

The Start event in the budding yeast cell cycle has traditionally been considered a point of commitment to the cell-division cycle with respect to cell growth and size control and mating factor treatment (Johnston et al., 1977). The issue of whether Start is appropriately considered as a hard transition, or instead as a graded series of temporally correlated events with relatively loose functional coupling, is unresolved (Cross, 1995; Dirick et al., 1995). Start coincides with, and may in part consist of, transcriptional activation of the G1 cyclins *CLN1* and *CLN2*, the B type cyclins *CLB5* and *CLB6*, and many other genes involved in early cell cycle events (Spellman et al., 1998). Induction requires activation of the Cdk Cdc28 by the G1 cyclin Cln3 (Dirick et al., 1995; Koch et al., 1996; Stuart and Wittenberg, 1995; Tyers et al., 1993). Cln3-Cdc28 promotes formation of the RNA polymerase II holoenzyme at the TATA boxes of target genes (Cosma et al., 2001). Overexpression or deletion of *CLN3* results in small or large cell size, respectively (Cross, 1988; Nash et al., 1988), presumably reflecting early or late activation of the transcriptional program ("early" or "late" relative to the cell size "clock"). Regulation of Start by Cln3 is dependent on the transcription factors Swi4/Swi6 (SBF) and Mbp1/Swi6 (MBF) (Wijnen et al., 2002). After transcriptional activation of the G1 cyclins *CLN1* and *CLN2*, Cln1,2-Cdc28 complexes drive activation of B type cyclins, bud emergence, and microtubule organizing center duplication (Cross, 1995; Dirick et al., 1995). The requirement for *CLN* proteins at Start may reflect a quantitative threshold (Schneider et al., 2004).

The Whi5 transcriptional repressor negatively regulates Start by binding to and inactivating SBF and perhaps MBF. Cln3-Cdc28 activates G1/S transcription in part by inhibitory phosphorylation of Whi5, resulting in release of SBF and export of Whi5 from the nucleus (Costanzo et al., 2004; de Bruin et al., 2004).

In the absence of *CLN3*, *CLN1* and *CLN2* are sufficient for transcriptional activation via positive feedback (Costanzo et al., 2004; Cross and Tinkelenberg, 1991; de Bruin et al., 2004; Dirick et al., 1995; Dirick and Nasmyth, 1991; Stuart and Wittenberg, 1995; Tyers et al., 1993): a basal level of Cln1,2 inactivates Whi5 and/or directly activates SBF/MBF, thus driving transcription of SBF/MBF target genes including *CLN1,2*. Basal activity of the *CLN1* or *CLN2* promoters may be provided by *BCK2* (Di Como et al., 1995; Epstein and Cross, 1994) or *RME1* (Toone et al., 1995).

The Start transition is important for cell size and growth rate control and coordination of growth and division (Jorgensen and Tyers, 2004). Budding yeast divide asymmetrically, with a larger mother and a smaller daughter; the daughters exhibit a much longer delay between mitosis and Start. This delay is in part due to the smaller size of daughters (Hartwell and Unger, 1977), but there must be other factors involved (Lord and Wheals, 1981); these may include the daughter-specific transcription factor Ace2 (Laabs et al., 2003).

By using time-lapse microscopy, substantial variability has been observed in cell cycle Start times (Hartwell and Unger, 1977; Lord and Wheals, 1981, 1983). These early studies, although very accurate and informative, were limited by the restriction to cytologically detectable cell cycle markers. Disruption of early G1 expression of Swi4 and Cln3 strongly increased population-level variability in cell size at which budding occurred (MacKay et al., 2001), suggesting that these regulators control cell-to-cell variability as well as overall levels of transcription of Swi4 target genes.

More recently, the issue of gene expression noise as indicated by cell-cell variability has been addressed in simple synthetic genetic circuits. Substantial variability was attributed to cell-wide variations in the efficiency of gene expression or to individual promoter-specific variations in frequency of transcription (Elowitz et al., 2002; Raser and O'Shea, 2004). Translation may amplify gene expression noise (Ozbudak et al., 2002). It is unclear as yet how these insights will play out in the occurrence and regulation of noise in more complex natural systems such as cell cycle regulation.

Here, we revisit the issue of variability (noise) in cell cycle Start. The 25 years since these issues were last addressed has provided us with the ability to extend the previous single-cell observations by using fluorescent proteins as markers of regulation of gene expression

*Correspondence: fcross@rockefeller.edu

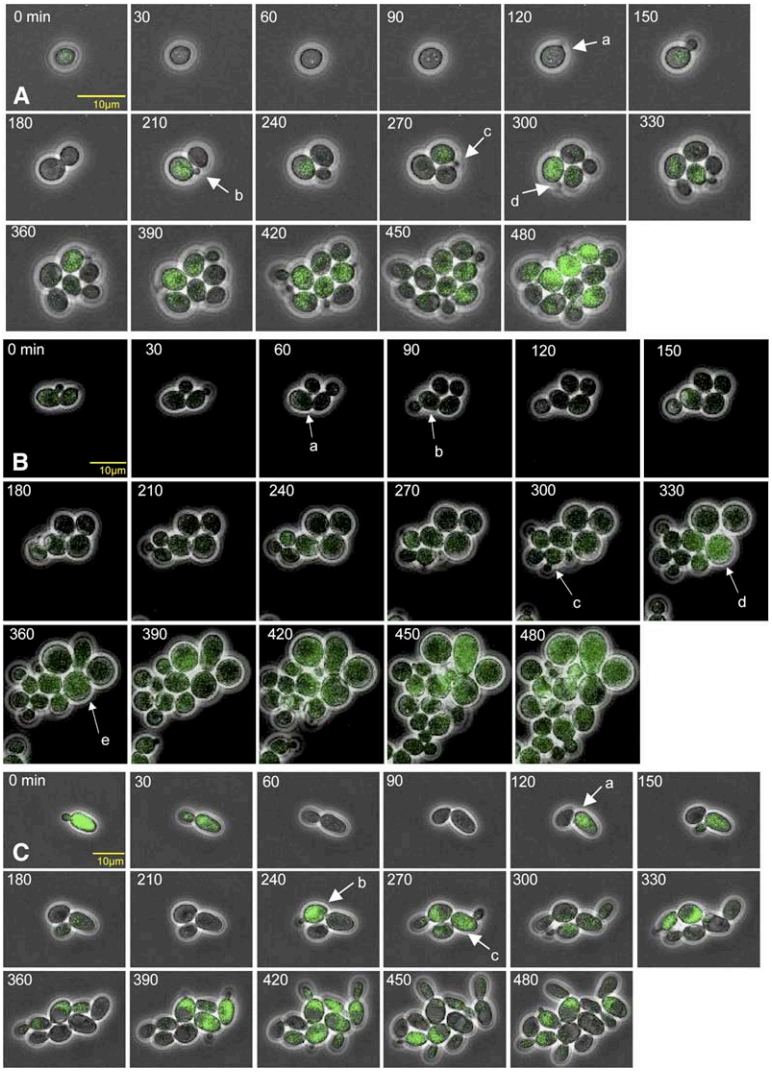

Figure 1. Composite Phase Contrast and *CLN2pr-GFP* Images in Three Strain Backgrounds

(A) Wt cells showing: (a) the first bud emergence accompanied by a burst of *CLN2pr-GFP* signal for the founder cell; (b) the second bud emergence accompanied by *CLN2pr-GFP* signal for the founder cell; (c) the first bud emergence with *CLN2pr-GFP* signal for the first daughter, illustrating the daughter delay; (d) the third bud emergence with *CLN2pr-GFP* signal for the founder cell.

(B) *swi4Δ* cells showing: (a and b) bud emergence without a robust burst of *CLN2pr-GFP* signal for the founder cell, demonstrating the decrease in amplitude of *CLN2pr-GFP* peaks associated with budding; (c) the second bud emergence for the mother indicated in (a and b) occurring 210 min after the first with normal *CLN2pr-GFP* expression associated; (d and e) budding accompanied by a robust burst of *CLN2pr-GFP* expression occurring 330 min after the first bud emergence for the cell (t = 0).

(C) *cln3 mbp1 rme1Δ* cells showing: (a) bud emergence with a very robust burst of *CLN2pr-GFP* signal for the founder cell, demonstrating the increase in amplitude of *CLN2pr-GFP* peaks associated with budding; (b) the first bud emergence for the first daughter (appears as a bud at t = 0) at t = 240 min, demonstrating the abnormal length of bud-bud intervals in the *cln3 mbp1 rme1Δ* strain; (c) budding accompanied by a robust burst of *CLN2pr-GFP* expression occurring 150 min after the previous bud emergence shown in (a). 10 micron size bars included; note that the mutant images are reduced due to large cell size.

or of structures involved in cell division and with genetic manipulations to accurately dissect Start regulation. Our results have implications for noise in gene regulation at the level of single genes as well as at the level of the whole Start program and for systems-level dynamics of Start regulation.

Results

Measurement of the G1/S Transcriptional Program in Individual Cell Cycles

Cell cycle initiation in budding yeast is marked by the induction of a transcriptional program of a battery of 119 genes (Spellman et al., 1998), including the G1 cyclin *CLN2*. To examine this program at the single-cell level, we employed a *CLN2pr-GFP* construct with destabilized GFP under control of the *CLN2* promoter, which exhibits cell-cycle-regulated expression at a population level (Mateus and Avery, 2000). We integrated this construct at the endogenous *CLN2* locus. This results in *CLN2pr-GFP* being regulated by the intact *CLN2* promoter, whereas the adjacent normal copy of *CLN2* is regulated by a truncated 614 bp promoter that should retain sufficient sequences to provide full expression and cell cycle regulation (Cross et al., 1994; Stuart and Wittenberg, 1994). It is important to note that *GFP* coding sequences replace *CLN2* coding sequences within the *CLN2pr-GFP* construct; this is a pure gene expression reporter that cannot on its own carry out any of the Cln2-specific Start activities.

We observed cell-cycle-regulated accumulation of fluorescence around the time of budding, which we could quantitate based on fluorescent signal intensity within the segment boundaries (Figures 1A and 2A). Diploid cells with one copy of *CLN2pr-GFP* attain fluorescence peaks that are approximately half the amplitude of diploids with two copies of the reporter, showing the quantitative nature of the marker (data not shown).

We correlated fluorescence from this reporter with accumulation of GFP protein in batch cultures synchronized by *cdc20* block release. Batch GFP protein accumulation peaks at a similar time as the peak in average fluorescence intensity in single cells measured at 15 min resolution (S. Di Talia and J.B., unpublished data), suggesting that folding to the fluorescent form occurs within about 15 min. *GFP* RNA peaks at a similar time after release as does endogenous *CLN2* RNA, and GFP protein accumulation follows ~15 min later

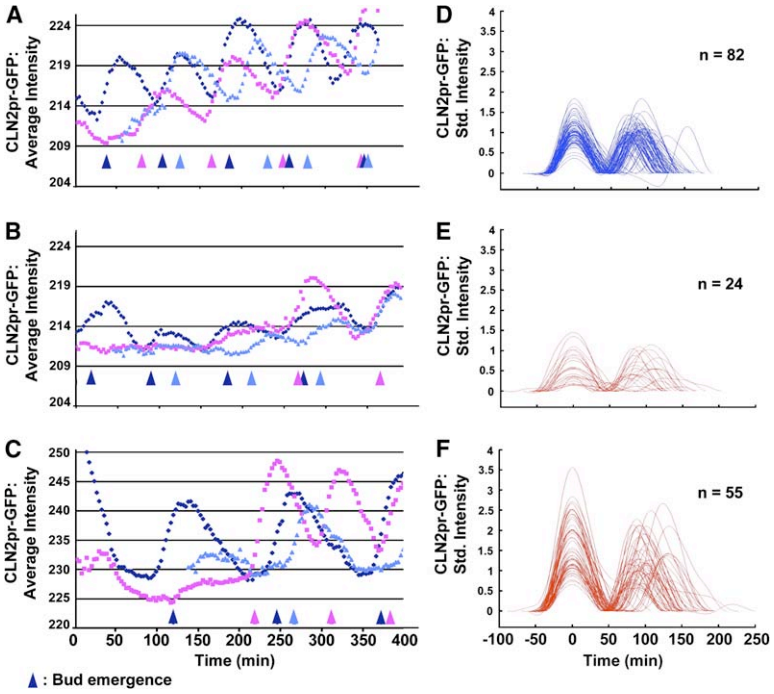

Figure 2. Sample Traces and Composite Peaks of *CLN2pr-GFP* for Wt, *swi4Δ*, and *cln3 mbp1 rme1Δ* Strains

(A) and (D), Wt; (B) and (E), *swi4Δ*; (C) and (F), *cln3 mbp1 rme1Δ*. The first column (A, B, and C) has the raw fluorescence averaged over the cellbodies as defined by the segmenter at 3 min time intervals, for several cells in a pedigree. The colored arrows define bud emergence for the corresponding trace. The second column (D, E, and F) shows the spline fit to the fluorescence data for all peak-to-peak pairs for which exact timing and amplitudes can be determined. Traces have been corrected by subtracting a baseline connecting flanking troughs, aligned with the first peak at zero, and graphed on a common scale (see also Figure S2).

(unpublished data). Therefore, the GFP signal is a good transcriptional reporter for initial activation of *CLN2* transcription, with about a 15 min lag. GFP signal persists for longer than *CLN2* RNA, presumably due to persistence of the destabilized GFP protein (with about a 45 min half-life; Mateus and Avery, 2000), but decays sufficiently to allow detection of the rise in the subsequent cell cycle.

CLN2pr-GFP thus provides a single-cell marker of the G1/S transcriptional program. At least one of *CLN1*, *CLN2*, *PCL1*, or *PCL2*, all of which are induced by the G1/S program, is required to induce bud emergence (Moffat and Andrews, 2004). As is noted above, the *CLN2pr-GFP* reporter is not a fusion protein and therefore does not itself induce budding. This allows us to examine the correlation and timing reliability of *CLN2pr-GFP* induction as measured by fluorescence and the firing of *CLN1*, *CLN2*, *PCL1*, and/or *PCL2* as indicated morphologically by bud emergence (Figure 1). *CLN2pr-GFP* induction and bud emergence are reliably coupled (Figures 2A and 3D). *CLN2pr-GFP* fluorescence peaks at a rather similar level in succeeding cell cycles (after subtraction of a variable but generally rising background level, which we observe with other GFP fluorescent markers [data not shown] and consider to be nonspecific, although we do not know its basis) (Figures 2D and 3A). We observe the expected delay of newly born daughters (see Introduction) for their first cycle of *CLN2pr-GFP* induction and budding (see Figure S3D in the Supplemental Data available with this article online). First-time and multitime ("experienced") mothers show similar mean and standard deviation for peak *CLN2pr-GFP* fluorescence and for time between budding and *CLN2pr-GFP* peak (Table S1), allowing the treatment of all mother cells as a single population.

This simple result of reliable correlation of *CLN2pr-GFP* induction and bud emergence (Figure 3D) indicates the simultaneous induction of multiple genes in the G1/S regulon. This determination uniquely requires single-cell analysis. The alternative hypothesis that, for example, *CLN1*, but not *CLN2*, might be activated in some individual cell cycles has never been evaluated previously but is largely ruled out here. This conclusion has implications for the dynamics of the G1/S transcriptional system, which we explore further below.

Recently, it was reported (Becskei et al., 2005) that regulation differed for two copies of a synthetic reporter gene when placed in a tandem array, as compared to placing the two copies at the same position on homologous chromosomes in a diploid. We were concerned that having *CLN2pr-GFP* in tandem to a functional *CLN2* gene might perturb our results, as we were assuming independent regulation of *CLN2pr-GFP* and genes inducing bud emergence, including *CLN2*. To test independence, we compared (1) *CLN2pr-GFP* in tandem with a disrupted *cln2* gene, in *trans* to a functional *CLN2* gene, against (2) *CLN2pr-GFP* in tandem with wild-type *CLN2* (as used in all other experiments in this paper), in *trans* to a disrupted *cln2* gene, in heterozygous diploids. We observed little difference in extent or timing of GFP accumulation relative to bud emergence when comparing these diploids (Table S2). This was also true when comparing the *cis* and *trans* configurations in a *cln1 cln3* diploid background, where the functional *CLN2* gene was specifically required to induce bud emergence (Table S2). These results suggest that *CLN2pr-GFP* and *CLN2* are independently regulated, even when they are present in a tandem array.

The Swi4 DNA Binding Protein Helps Maintain a Low-Noise G1/S Program

The G1/S transcriptional program is driven by Swi4/Swi6 (SBF) and Mbp1/Swi6 (MBF) (see Introduction). These two transcription factors largely overlap for the regulation of most genes, at least at a population level, probably due to the ability of both factors to bind to promoters

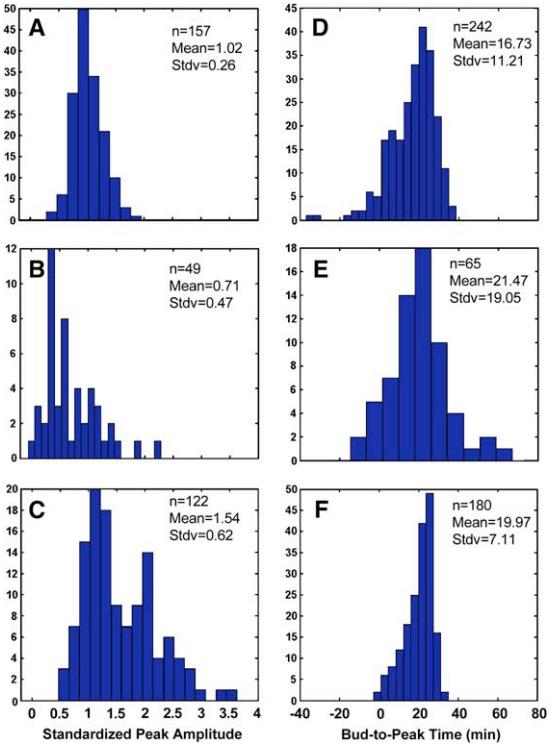

Figure 3. Histograms of *CLN2pr-GFP* Peak Heights and Bud-to-Peak Times for Wt, *swi4Δ*, and *cln3 mbp1 rme1Δ* Strains

(A) and (D), Wt; (B) and (E), *swi4Δ*; (C) and (F), *cln3 mbp1 rme1Δ*. Peak heights in the first column (A, B, and C) are in compatible units scaled to make the mean of Wt 1. The times in the second column (D, E, and F) are in minutes. For (E), there is one outlier at 120 min that is not shown. This outlier actually represents a larger class of events in the *swi4* strain of cells with very long delays between budding and the *CLN2-GFP* peak that were excluded from our quantitative analysis because of the lack of a clearly detectable minimum in fluorescence after the peak (see Supplemental Data for details of data analysis).
(A–C) Peak amplitudes for *CLN2pr-GFP.*
(D–F) Time (min) from budding to *CLN2pr-GFP* peak (bud-to-peak times).

of most of these genes (Bean et al., 2005). This apparent overlap in function leads to the question of whether the two factors simultaneously activate transcription in all promoters in every cell, or, alternatively, whether some cells use one factor and others another, at each individual coregulated gene. This distinction cannot be made at the population level. Because *CLN2* is thought to be regulated by both Swi4 and Mbp1 binding (Stuart and Wittenberg, 1994), we tested the requirements for Swi4 and Mbp1 for *CLN2pr-GFP* expression and correlated budding at the single-cell level.

Deletion of *mbp1* had little or no effect on timing or reliable cooccurrence of *CLN2pr-GFP* expression or budding (data not shown). In contrast, deletion of *swi4* had remarkable effects.

We quantitated peak *CLN2pr-GFP* expression levels after background subtraction and standardization (see Experimental Procedures) in *swi4* mutants compared to wild-type and found that the average peak level for *swi4* was reduced to about 70% of the wild-type average peak level (Figure 3B; Table 1). This reduction in *CLN2pr-GFP* expression due to *swi4* deletion ($p < 0.0005$) was expected from previous results (Koch and Nasmyth, 1994).

What could not have been anticipated from previous population-level measurements was that the *swi4* cells also exhibit significantly greater variation in *CLN2pr-GFP* expression ($p < 0.01$ when comparing coefficients of variation; Table 1). The consequence is that individual *swi4* cells exhibit a *CLN2pr-GFP* peak around the time of bud emergence varying from almost undetectable to essentially wild-type (wt) in magnitude.

Another measure of the disruption of coherence of the Start transition in *swi4* cells is the increased variability in the time between bud emergence and the *CLN2pr-GFP* peak (Figure 3E; Table 1). The mean increased modestly, but the standard deviation grew by almost a factor of two (19 min in *swi4* versus 11 in wt; $p < 0.01$ by F test). A careful statistical analysis (Table 1 legend) indicates that this effect does not result from occasional outliers but rather reflects a frequent defect in coherence of the cell cycle in the absence of Swi4. This conclusion is confirmed by the pedigree analysis reported below.

These *swi4* phenotypes were generally more severe in first-time mothers than in experienced mothers (Table S1); this observation is interesting, because there was no discernable difference between first-time and experienced *SWI4* mothers.

The lower and more variable *CLN2pr-GFP* expression and the loss of temporal coherence between two aspects of the Start program (*CLN2pr-GFP* and budding) due to *swi4* deletion both argue that Swi4 is a critical integrator to keep Start robust and coherent, despite the presence of a reasonably active Mbp1-dependent backup pathway for Swi4-independent expression of most genes in the Start and G1/S regulon (Bean et al., 2005).

We examined the effect of ectopically expressing *CLN2* from an integrated *MET3-CLN2* (Met-repressible promoter) on the *swi4* cell cycle. This construct can bypass the requirement for almost the entire G1/S transcriptional program, because it rescues viability of cells deleted for the major redundant transcription factors for this program, *SWI4* and *MBP1* (Koch et al., 1993; Bean et al., 2005). In a *SWI4-wt* background, *MET3-CLN2* moderately reduced peak *CLN2pr-GFP* expression to 74% of wt (Figure 4C; Table 2), indicating that Swi4/Mbp1-dependent expression can still function reasonably well with *CLN2* being expressed constitutively. (Note that all comparisons for experiments involving *MET3-CLN2* were done with wt cells lacking *MET3-CLN2* but grown on −Met medium, controlling for a moderate increase in doubling time due to −Met medium; data not shown). In contrast, in a *swi4* background, *MET3-CLN2* strikingly reduced *CLN2pr-GFP* expression in many cell cycles (peak values relative to wt of 16% ± 20%, with almost half of the cell cycles lacking any significant peak; Figure 4D; Table 2). *MET3-CLN2* expression drives early budding and cell cycle initiation (Dirick et al., 1995); thus, forcing early Start by *MET3-CLN2* expression is highly antagonistic to *CLN2pr-GFP* expression, at least in the absence of Swi4.

Swi4 Helps Maintain Cell Size and Budding Regularity

swi4 cells are large on average (Jorgensen et al., 2002). We noted extreme variability in *swi4* cell size in time-lapse. Very large cells were frequently generated in the course of the experiment from cells of near-normal

Table 1. Peak *CLN2-GFP* Levels and Time from Budding to *CLN2-GFP* Peak in Wt, *swi4*, *cln3 mbp1 rme1*, *whi5*, *swi4 whi5,* and *cln3 mbp1 rme1 whi5*

Peak Amplitude CLN2-GFP[a]						
	wt	*swi4*	*cln3 mbp1 rme1*	*whi5*	*swi4 whi5*	*cln3 mbp1 rme1 whi5*
Mean	1.02	0.71	1.54	0.90	0.62	1.32
Standard deviation	0.26	0.47	0.62	0.33	0.29	0.37
n	157	49	122	127	44	51
Coefficient of variation	0.25	0.66	0.40	0.37	0.47	0.28
Difference of mean, mutant versus wt (t test)	NA	$p < 0.0005$ (decreased)	$p < 0.0005$ (increased)	$p < 0.0005$ (decreased)	NA	NA
Difference of standardized variability, mutant versus wt	NA	$p < 0.01$ (increased)	$p < 0.01$ (increased)	$p < 0.01$ (increased)	NA	NA
Mean, *whi5* versus *WHI5+* (t test)	NA	NA	NA	$p < 0.0005$ (decreased)	$p > 0.1$ (unchanged?)	$p < 0.005$ (decreased)
Standardized variability, *whi5* versus *WHI5+*	NA	NA	NA	$p < 0.01$ (increased)	$p < 0.025$ (decreased)	$p < 0.01$ (decreased)
Mean, *swi4* versus *SWI4+* (t test)	NA	$p < 0.0005$ (decreased)	NA	NA	$p < 0.0005$ (decreased)	NA
Standardized variability, *swi4* versus *SWI4+*	NA	$p < 0.01$ (increased)	NA	NA	$p < 0.05$ (increased)	NA
Time from Budding to CLN2-GFP Peak Time (min)						
	wt	*swi4*	*cln3 mbp1 rme1*	*whi5*	*swi4 whi5*	*cln3 mbp1 rme1 whi5*
Mean	16.7	21.5	20.0	15.3	13.5	18.5
Standard deviation	11.2	19.0	7.1	11.3	13.5	8.2
n	242	65	180	212	61	79
Coefficient of variation	0.67	0.89	0.36	0.74	1.00	0.44
Difference of mean, mutant versus wt (t test)	NA	$p < 0.05$ (increased)	$p < 0.0005$ (increased)	$p < 0.1$ (decreased?)	NA	NA
Difference of standardized variability, mutant versus wt	NA	$p < 0.01$ (increased)	$p < 0.01$ (decreased)	$p < 0.1$ (increased?)	NA	NA
Mean, *whi5* versus *WHI5+* (t test)	NA	NA	NA	$p < 0.1$ (decreased?)	$p < 0.005$ (decreased)	$p < 0.1$ (decreased?)
Standardized variability, *whi5* versus *WHI5+*	NA	NA	NA	$p < 0.1$ (increased?)	$p > 0.1$ (unchanged?)	$p < 0.05$ (increased)
Mean, *swi4* versus *SWI4+* (t test)	NA	$p < 0.05$ (increased)	NA	NA	$p > 0.1$ (unchanged?)	NA
Standardized variability, *swi4* versus *SWI4+*	NA	$p < 0.01$ (increased)	NA	NA	$p < 0.01$ (increased)	NA

GFP signal was quantitated, thresholded, background-subtracted, and standardized to wt. Bud emergences were assigned to GFP peaks, and the time difference from budding to peak was calculated. All calculations were performed automatically by the analysis software with the segmented and annotated data files as input. Mean, standard deviation, number of observations (n), and coefficient of variation (standard deviation divided by mean) are shown. Statistical significance of difference between means is reported as a p value based on a t test, using a pooled variance estimate. A standard Student's t test was used for comparison of sets with equal variances, whereas a Welch's t test was used in the case of unequal variances. Statistical significance of difference between coefficients of variation is reported as a p value based on an F test (ratio of squared coefficients of variation). The effect of the mutation on mean or variation is indicated in parentheses after the p value; a question mark indicates a p value above the standard 0.05 level. The effects on the differences between means and coefficients of variation for the various mutants shown above were not significantly affected by trimming the data to remove data points that lay more than three standard deviations away from the mean (data not shown); thus rare outliers were not responsible for these statistical effects.

[a] Arbitrary Units

size, due to extensive and variable cell cycle delays (Figure 5A).

To analyze this phenotype more closely, we examined pedigrees of wt and *swi4* stains with integrated *CDC10-GFP* (septin ring marker) (Park et al., 2003). The Cdc10-GFP ring appears at bud emergence and fades rapidly upon cytokinesis due to mitotic cyclin proteolysis (Cross et al., 2005). Wt pedigrees, based on division-to-division times deduced from Cdc10-GFP ring disappearance, are fairly regular, with a slant due to daughter delay (Figure 5B). In contrast, *swi4* pedigrees are much more variable with mixtures of normal-sized and extremely long branches. These long delays cause increased cell size (data not shown), as expected if cell growth continues independent of the cell division cycle (Johnston et al., 1977). These long delays in *swi4* cells are almost invariably associated with the interval between cytokinesis and the next bud emergence; the subsequent interval between budding and cytokinesis is affected little by *swi4* deletion (data not shown). The delays are frequently accompanied by multiple abortive septin rings at the cell cortex (Figure 5A), suggesting some ability to initiate, but not complete, the normal budding program in the absence of Swi4. In some cases, these large cells undergo regular cell cycles after periods of delay, suggesting reversibility. Ectopic expression of *CLN2* with integrated *CLN3pr-CLN2* largely rescues the *swi4* pedigree phenotype (Figure 5B), indicating that the aberrant

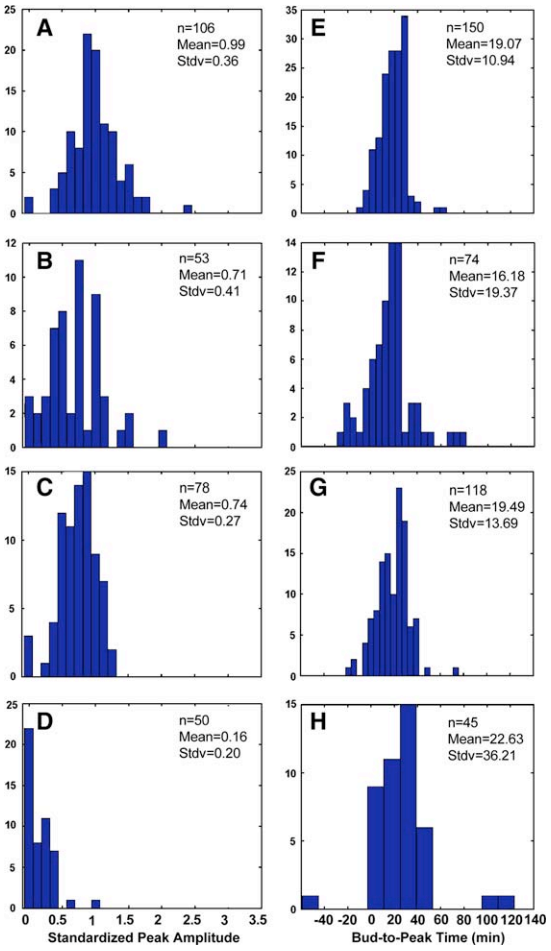

Figure 4. Histograms of *CLN2pr-GFP* Peak Heights and Bud-to-Peak Times in Wt and *swi4Δ*, with and without *MET3-CLN2* Expression

Analysis is as in Figure 3. (A) and (E), Wt; (B) and (F), *swi4Δ*; (C) and (G), *MET3-CLN2*; (D) and (H), *swi4Δ MET3-CLN2.* Adding constitutive *CLN2* expression from *MET3-CLN2* in a *SWI4* background slightly attenuates and decorrelates the peaks ([A] and [E] versus [B] and [F]), whereas constitutive *CLN2* in a *swi4Δ* background strongly reduces peak intensity (D). One outlier at –150 min in the bud-to-peak histogram in (H) is not shown. (A), (B), (C), and (D) indicate peak amplitudes for *CLN2pr-GFP*; (E), (F), (G), and (H) indicate time (min) from budding to *CLN2pr-GFP* peak (bud-to-peak times).

pedigrees in *swi4* cells can be attributed to failure to activate *CLN2* or functionally related genes.

Because *swi4* deletion affects cell-wall morphogenesis (Igual et al., 1996), we asked if the large *swi4* cells could be due to osmotic swelling and thus suppressible by growth in high-osmotic-strength medium. A similar size distribution of *swi4* mutants in the presence or absence of 1M sorbitol was observed by Coulter counter analysis, making this interpretation unlikely (data not shown).

Although we cannot fully interpret these sporadic extended, unbudded periods in *swi4* mutants, the phenomenon clearly supports the idea that removal of Swi4 strongly increases variability in some aspects of the G1/S program, as concluded from the quantitative study of *CLN2pr-GFP* expression.

Sufficiency of Swi4 to Ensure Reliable Correlated Expression of the G1/S Regulon

swi4 strains are dependent on a number of accessory proteins for viability. In the W303 background, *swi4* is synthetically lethal with a single deletion of *cln3*, *mbp1*, or *rme1*, all of which have been implicated in activation of G1/S-regulated transcription (see Introduction). In contrast, in a *SWI4* background, all three of these genes can be simultaneously deleted. Figures 1C, 2C, 2F, 3C, and 3F show quantitative analysis of *CLN2pr-GFP* expression in the *cln3 mbp1 rme1* background. In contrast to the results with *swi4*, we observed that *cln3 mbp1 rme1* strains exhibited no reduction in *CLN2pr-GFP* induction (Table 1); in fact, our quantitation suggested an ~1.5-fold greater than wt peak *CLN2pr-GFP* induction ($p < 0.0005$). Also in contrast to *swi4*, the variability of the timing between bud emergence and peak *CLN2pr-GFP* induction was significantly reduced in *cln3 mbp1 rme1* compared to wt (coefficient of variation of 0.36 for the mutant compared to 0.67 for wt; $p < 0.01$).

Thus, whereas removal of Swi4 decreases *CLN2pr-GFP* expression and increases variability in both *CLN2pr-GFP* expression and its timing relative to bud emergence (marking induction of endogenous G1 cyclins), removal of Cln3, Mbp1, and Rme1 has the opposite effects.

What is occurring in the *cln3 mbp1 rme1* background? In wt cells, the transcriptional program is assumed to be initiated primarily by Cln3 inactivating Whi5, resulting in release of Swi4-Swi6 and subsequent activation of transcription. Although the *CLN1* and *CLN2* targets of this pathway have the potential to activate their own transcription (Cross and Tinkelenberg, 1991; Dirick and Nasmyth, 1991), this positive feedback activation is not thought to contribute strongly to the timing of initial *CLN1,2* induction (Dirick et al., 1995; Stuart and Wittenberg, 1995). In the *cln3 mbp1 rme1* context, though, there is no Cln3 for initial phosphorylation of Whi5/Swi4/Swi6. (Deletion of *MBP1* and *RME1* eliminate other Swi4-backup pathways, simplifying the system). Therefore, we assume that these cells are acting in positive feedback mode: a low level of expression of *CLN1* or *CLN2* inactivates Whi5 and activates Swi4-Swi6, leading to a rapid and efficient ramping up of expression. Supporting this hypothesis, *CLN2pr-GFP MET3-CLN2 cln1 cln2 cln3* strains arrested by turnoff of *MET3-CLN2* fail to exhibit high *CLN2pr-GFP* expression for many cell cycle times, indicating that *CLN2pr-GFP* expression is dependent on expression of at least one *CLN* gene.

Thus, this positive-feedback mode of activation of the G1/S regulon may result in a tightly coordinated and efficient expression once activation is achieved; surprisingly, expression is even more efficient and coordinated than in wt, in which the positive feedback mode is much less functional.

The time of induction in such a positive-feedback system should be delayed (because an activator is missing) and probably more variable if the feedback induces bistability. With strong feedback, activation may occur via rare fluctuations in the *CLN2* message level that lead to sustained Cln2 production. *cln3 mbp1 rme1* cells have a significantly increased doubling time (e.g., analyzing the average time between successive bud emergence in mothers gives 91 min for wt and 118 for the mutant;

Table 2. Peak *CLN2-GFP* Levels and Time from Budding to *CLN2-GFP* Peak in Wt versus *MET3-CLN2* versus *swi4* versus *swi4 MET3-CLN2*

Peak Amplitude CLN2-GFP[a]				
	wt	*MET3-CLN2*	*swi4*	*swi4 MET3-CLN2*
Mean	0.99	0.74	0.71	0.16
Standard deviation	0.36	0.27	0.41	0.20
n	106	78	53	50
Coefficient of variation	0.36	0.36	0.58	1.25
Mean, with *MET-CLN2* versus without *MET-CLN2* (t test)	NA	$p < 0.0005$ (decreased)	NA	$p < 0.0005$ (decreased)
Standardized variability, with *MET-CLN2* versus without *MET-CLN2*	NA	$p > 0.5$ (unchanged)	NA	$p < 0.01$ (increased)
Mean, *swi4* versus wt (t test)	NA	NA	$p < 0.0005$ (decreased)	$p < 0.0005$ (decreased)
Standardized variability, *swi4* versus wt	NA	NA	$p < 0.01$ (increased)	$p < 0.01$ (increased)
Time from Budding to CLN2-GFP Peak Time (Min)				
	wt	*MET3-CLN2*	*swi4*	*swi4 MET3-CLN2*
Mean	19.1	19.5	16.2	22.6
Standard deviation	10.9	13.7	19.4	36.2
n	150	118	74	45
Coefficient of variation	0.57	0.70	1.20	1.60
Mean, with *MET-CLN2* versus without *MET-CLN2* (t-test)	NA	$p > 0.5$ (unchanged)	NA	$p < 0.2$ (increased?)
Standardized variability, with *MET-CLN2* versus without *MET-CLN2*	NA	$p < 0.05$ (increased)	NA	$p < 0.025$ (increased)
Mean, *swi4* versus wt (t-test)	NA	NA	$p < 0.2$ (decreased?)	$p > 0.2$ (unchanged?)
Standardized variability, *swi4* versus wt	NA	NA	$p < 0.01$ (increased)	$p < 0.01$ (increased)

All measurements were made on Met-free medium (to induce *MET3-CLN2* where present). Data analysis as in Table 1, including analysis of outlier exclusion. Note that this data set includes two independent *swi4* versus *SWI4* comparisons (on Met-free medium, with or without *MET3-CLN2*) that confirm the conclusions from Table 1 that *swi4* deletion decreases *CLN2-GFP* peak level whereas increasing peak level variability and also increasing variability of the time from bud emergence to peak occurrence.
[a] Arbitrary Units

$p < 0.0005$; Figures S3A and S3C), with an apparent 12% increase in standardized variability ($p < 0.1$). Increased variability in timing for cells in positive-feedback mode can be more clearly detected in our analysis of nuclear localization of the Whi5 transcriptional repressor, as described below, because this analysis focuses attention on the critical interval between cell division and Start.

Regulation of Nuclear Localization of the Whi5 Transcriptional Repressor

Phosphorylation of Whi5 and SBF/MBF components by cyclin-Cdk complexes release Whi5 from SBF/MBF, driving transcriptional activation and Whi5 nuclear exit (Costanzo et al., 2004; de Bruin et al., 2004). We analyzed the timing of nuclear entry and exit of the Whi5-GFP fusion protein, expressed from the endogenous locus (Costanzo et al., 2004), correlated with budding (Figure 6). Mother cells exhibited only a short (~5–15 min) period of Whi5-GFP nuclear residence, whereas daughter cells retained Whi5 in the nucleus for a longer and more variable period (~10–60 min) (Figure 6D). Budding followed Whi5-GFP nuclear exit by ~30 min, with essentially no asymmetry between mothers and daughters (Figure 6E). Completion of mitosis as indicated by Whi5-GFP nuclear reentry occurred a variable time period later (~60 min), at which time Whi5-GFP reliably entered both mother and daughter nuclei simultaneously (Figure 6C). This simultaneity likely is a consequence of the mother and daughter nuclei sharing common cytoplasm until mitotic exit, the requirement for Whi5-GFP nuclear entry (Costanzo et al., 2004). Whi5-GFP localization thus marks critical cell cycle events: nuclear entry due to catastrophic Cdk inactivation upon completion of mitosis and nuclear exit due to Cdk reactivation. Consistent with this picture, Whi5-GFP remains nuclear for many hours in cells blocked in G1 with low Cdk activity levels due to removal of the three G1 cyclins, *CLN1*, *CLN2*, and *CLN3*.

We examined Whi5-GFP localization in the positive-feedback context described above (*cln3 mbp1* background; additional deletion of *rme1* did not significantly change these results [data not shown]). Compared to wt, this strain exhibited variable but sometimes very long delays specifically in the interval during which Whi5-GFP was nuclear (Compare Figures 6A and 6B; Figure 6D). *cln3 mbp1 rme1* cells are significantly larger than wt cells (Figures 1C and 6B), and the long G1 delays with nuclear Whi5-GFP were reproducibly associated with significant cell growth, sometimes to a very large size (Figure 6B; data not shown), although we did not try to quantitate this effect. Once Whi5-GFP nuclear exit was attained, the timing of the rest of the cell cycle (Whi5-GFP nuclear exit to budding, and budding to Whi5-GFP nuclear reentry) was comparable to wt (Figures 6C and 6E). In all cases (mother and daughter, deletion strain and wt), the nuclear Whi5-GFP times could be approximately fit by a γ distribution, $t^a \exp(-t/b)$, with a in the range of two to three, and the time scale b variable to capture the range of times visible in Figure 6D (data not shown).

Whi5-GFP localization was hard to analyze definitively in *swi4* cells due to their frequent extreme morphological abnormalities, but lengthy delays before budding in the *swi4* background frequently occurred after Whi5-GFP nuclear exit (data not shown), in contrast to results with the *cln3 mbp1* background. This is plausible because

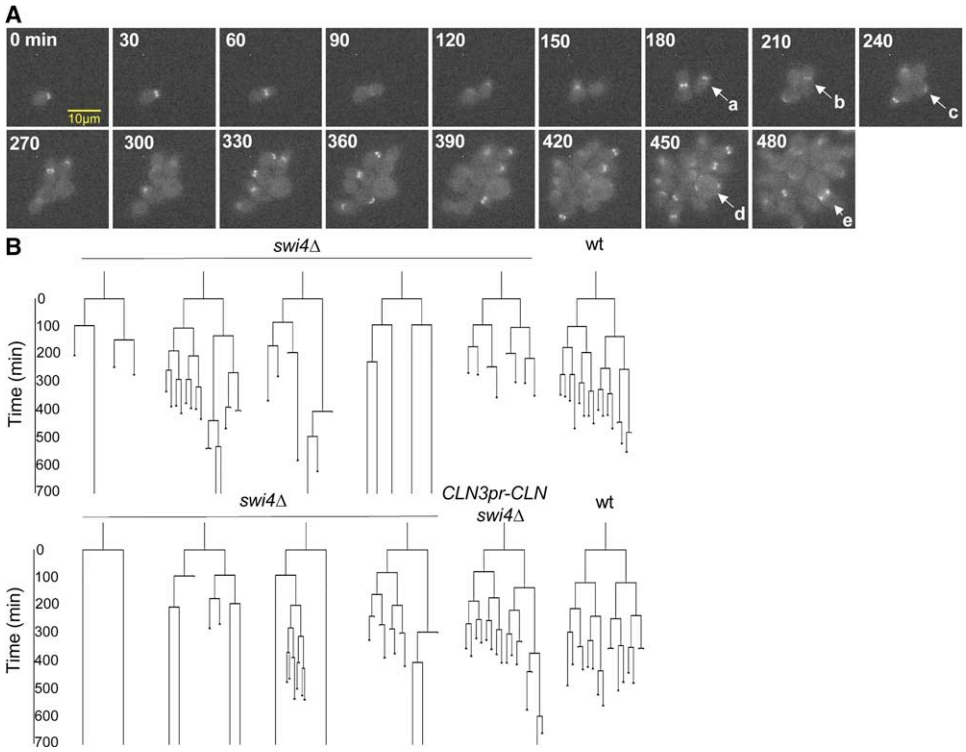

Figure 5. Erratic Pedigrees and Septin Ring Formation Due to *swi4* Deletion

(A) Fluorescent images of a *CDC10-GFP swi4Δ* strain grown under 3 min interval time-lapse conditions. (a) Cdc10 ring formation at bud emergence; (b) Cdc10 ring at the bud neck prior to division; (c) remnants of the Cdc10 ring after division; (d) multiple, simultaneous, abortive attempts to form a septin ring after a 210 min interval since the last division; (e) a single, functioning septin ring at the bud neck.

(B) Pedigrees. Branch points mark division (Cdc10-GFP ring splitting and/or fading); mothers to the left. Pedigrees go to 700 min or until cell stacking made the movie unreadable. A representative pedigree of *swi4 CLN3pr-CLN2* is also shown.

Whi5-GFP phosphorylation and inactivation in the *swi4* strain could be predicted to have little effect, because Swi4 is likely the main target of negative regulation by Whi5 (Costanzo et al., 2004; de Bruin et al., 2004).

The Role of Whi5 in Start Coherence

The repressive effects of Whi5 on SBF/MBF-mediated transcriptional activation (Costanzo et al., 2004; de Bruin et al., 2004) could be required to prevent premature firing. We tested the effect of removal of Whi5 on the activation of the *CLN2pr-GFP* reporter. *WHI5* deletion caused a lower and more variable peak of expression (mean amplitude 0.90 *whi5* versus 1.02 wt, $p < 0.005$; 48% increase in standardized variability in *whi5* compared to wt, $p < 0.01$; Table 1). *WHI5* deletion in a *cln3 mbp1 rme1* background caused a reduction in the increased *CLN2pr-GFP* amplitude seen in *cln3 mbp1 rme1* cells (1.32 *cln3 mbp1 rme1 whi5* versus 1.54 *cln3 mbp1 rme1*, $p < 0.005$; Table1) and a 22% increase in the variability in bud-to-peak timing ($p < 0.05$; Table 1).

We also tested the effects of *WHI5* deletion in a *swi4* background, and we were somewhat surprised to see detectable effects (Table 1), as one model predicted little effect because Swi4 appears to be the main target of the repressive effect of Whi5 (Costanzo et al., 2004; de Bruin et al., 2004). Some evidence for interaction between Whi5 and MBF was reported, though (Costanzo et al., 2004), and it is likely that the effects seen here will not be fully understood until Mbp1 regulation is clarified.

Discussion

Markers to Examine the Start Program

We have used time-lapse microscopy to collect phase-contrast and fluorescent images of yeast cells as they grow from a founder cell to a colony of 20–30 cells (at which time they cease to remain planar, limiting the yield of further information). Multiple fluorescent markers were used to examine the coherence of the Start phase in the division cycle in both wt and mutant cells. In contrast to compiling statistics from a static image of a field of cells, time-lapse recording provides temporal correlations between events cell by cell and permits a reassessment of linkages and subprograms that were previously defined by genetics and epistasis.

We have exploited three markers, *CLN2pr-GFP*, Cdc10-GFP, and Whi5-GFP. *CLN2pr-GFP* involves de novo transcription-translation, with a degradation tag that destabilizes the reporter so that periodic expression within the timescale of a cell cycle can be detected (Mateus and Avery, 2000). This marker provides a direct readout of the Start transcriptional program in single cells. The other markers functioned by relocation to the bud neck and nucleus, respectively, and relocation occurs on the order of the 3 min resolution used in this study.

Whi5 relocation allows for a very natural handle on a process central to cell cycle progression. Nuclear residence of Whi5 reflects a low-Cdk activity state, as Cdk

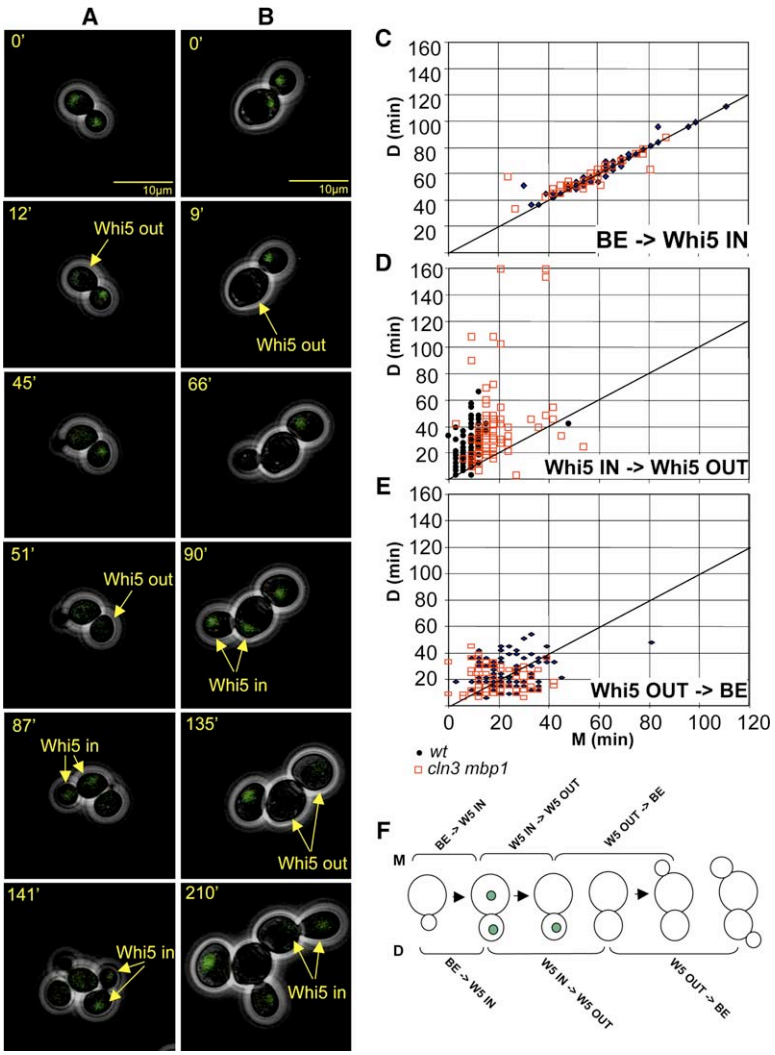

Figure 6. Whi5-GFP Nuclear Residence in Wt and *cln3Δ mbp1Δ*

(A) Composite phase-contrast and fluorescent images of a wt strain expressing *WHI5-GFP* under 3 min interval time-lapse conditions.

(B) Composite images of Whi5-GFP in *cln3Δ mbp1Δ* cells.

(C–E) Scatter of times for correlated mother (M) and daughter (D) pairs (from single cell divisions).

(C) Time between bud emergence (BE) and Whi5-GFP appearing in each newly divided nucleus (Whi5 IN).

(D) Time between Whi5-GFP appearing in the nucleus and disappearing from the nucleus (Whi5 OUT).

(E) Time between Whi5-GFP disappearing from the nucleus and bud emergence. In all graphs, the line for M = D is graphed; most points in the middle graph are above this line, indicating mother-daughter asymmetry in Whi5-GFP nuclear residence.

(F) Diagram showing these intervals.

phosphorylation leads to exit of Whi5 from the nucleus (Costanzo et al., 2004). In addition, nuclear Whi5 is at least partially causal in maintaining the low-Cdk activity state (Costanzo et al., 2004; de Bruin et al., 2004). It is striking that nuclear entry and exit of Whi5 correspond to the transition points for the "relaxation oscillator" proposed to control the budding yeast cell cycle (Cross, 2003).

Cdc10-GFP ring appearance marks bud emergence, and disappearance marks cytokinesis, which is not directly visualizable except by special microscopic conditions (Lord and Wheals, 1981).

We therefore have multiple fluorescent markers for Start-related processes, in addition to the classical one of bud emergence, suitable for single-cell analysis. These markers applied to wild-type and mutants have allowed us to distinguish variability in Start timing from variability in intra-Start coherence.

Control of Variability in Start Timing

It is a long-standing observation that mothers have a shorter G1 period than daughters (see Introduction). Here, we show that mother-daughter asymmetry in G1 is almost entirely confined to the cell cycle interval during which Whi5 is nuclear. Although there is a variable period that follows between Whi5 nuclear exit and budding, this time is not significantly longer in daughters than it is in mothers and may simply reflect variability in time required for bud assembly. In addition, the variability in cell cycle lengths due to *cln3 mbp1* deletion is almost entirely attributable to variability in Whi5 nuclear residence. This variability may be analogous to the extended G1 period, particularly of daughter cells, when grown in poor media. In that sense it is "natural" and external to the Start program itself.

cln3 mbp1 cells presumably operate in positive-feedback mode (see above). Such positive-feedback circuitry is likely to lead to considerable variability in time to firing. This qualitatively has the effect of accentuating the bistability between the Clb2-off, Sic1-high state pre-Start and the Clb2-on, low-Sic1 state post-Start (Cross, 2003; Nasmyth, 1996). There is no activation of *CLN1/2* until the cell is overly large, and then small cell-to-cell or environmental differences trigger activation. The G1 state does not lose its stability in a controlled way by ramping up Cln3 but acts as an amplifier of exogenous perturbations. In this bifurcation and bistability model, the additional deletion of *WHI5* is predicted to mute

the positive feedback of *CLN1/2*. We do indeed observe reduced amplitude of *CLN2pr-GFP* spikes in *whi5* mutants (Table 1); a full quantitative treatment of this situation is a subject for future work. The association between Whi5 nuclear exit and activation by SBF probably makes this transition largely irreversible, so the ultimate intensity of *CLN1/2* expression in the on state may not depend on whether *CLN3* is present (contrary to assumptions in Dirick et al., 1995).

Modeling a simplified version of this circuit by stochastic differential equations (J. Skotheim and E.D.S., unpublished data) indicates that increased timing variability due to the absence of *CLN3* can easily be obtained with plausible assumptions about the system. Although such models are only valuable as a rough guide, before such key assumptions can be tested empirically, the modeling does show "proof of principle" that lack of the Cln3 forcing trigger can lead to increased timing variability as well as an increased average delay while still producing high amplitude peaks when firing occurs.

The high-timing variability in transcriptional onset for this background means that the apparent low level of expression of target genes in synchronized bulk populations of *cln3* mutants (Dirick et al., 1995) could well be an artifact of loss of synchrony due to lack of the Cln3 external driver rather than due to low level of expression once it is activated. This is a conclusion that can only be reached by single-cell analysis.

Control of Intra-Start Coherence

swi4 mutants exhibit noise qualitatively distinct from the "timing" noise in the *cln3 mbp1 rme1* background, involving loss of robust expression from an internal component of the Start module and temporal decorrelation between two such markers (*CLN2pr-GFP* peak intensity and its lag after budding). The activation of SBF (and probably MBF) occurs in a two-step process in which, beginning at exit from mitosis into G1, the promoters are loaded with the component proteins of these complexes along with Whi5 (Cosma et al., 1999; Costanzo et al., 2004; de Bruin et al., 2004; Koch et al., 1996). Gene activation then occurs by phosphorylating the preassembled complexes. This is an admirable way of achieving synchronous firing of many promoters in one cell, provided sufficient waiting time and rapid phosphorylation. In the absence of Swi4, *CLN2pr-GFP* firing is dependent on Mbp1 binding alone, and this is likely less efficient, as DMS interference shows little binding to the *CLN2* promoter in the absence of Swi4 (Koch et al., 1996). Thus, in *swi4* mutant cells, a waiting period of normal duration may not allow efficient loading of Mbp1 onto the full set of SBF/MBF targets. Forcing Start, for example by expression of *CLN2* from the *MET3* promoter to artificially shorten the waiting period (Dirick et al., 1995), should strongly exacerbate this problem, consistent with our observation of nearly complete ablation of *CLN2pr-GFP* expression specifically in *MET3-CLN2 swi4* cells. Conversely, delaying Start, for example in the *cln3 mbp1* context give rise to the enhanced or in the natural context of long G1 in poor nutrient conditions, could allow additional time for complex assembly and thus synchrony and increased GFP intensity that we observed. Kato et al. (2004) have noted this "wait-then-activate" architecture for a number of cell cycle transitions in addition to G1/S genes controlled by SBF/MBF.

It is important that the period during which SBF/MBF can load on promoters is limited by mitotic B type cyclin activity (Amon et al., 1994; Koch et al., 1996), so cells that miss the natural loading window between mitotic exit and Start have little opportunity to correct the error. This may account for the strong effect of *MET3-CLN2*, especially in a *swi4* background.

The analysis of the consequences of *WHI5* deletion (Table 1) is, in general, consistent with the scheme to explain noise regulation in wt and the *cln3 mbp1 rme1* mutant. If Whi5 is acting to prevent early firing of *CLN2pr-GFP* before the *CLN2* promoter is fully loaded, then its deletion should result in lower expression with greater cell-to-cell variability and also possibly some loss of Start coherence as measured by budding-GFP peak time variability; all of these effects were observed. Whi5 also appears to be required for the full positive-feedback effect that we deduced to be occurring in the *cln3 mbp1 rme1* cells, as the quadruple *cln3 mbp1 rme1 whi5* mutant similarly exhibits reduction in peak amplitude and loss of Start coherence compared to the triple *cln3 mbp1 rme1* mutant. These effects of *WHI5* deletion are real but incomplete, presumably reflecting additional controls redundant with Whi5, such as were deduced previously (Costanzo et al., 2004; de Bruin et al., 2004).

Extrinsic and Intrinsic Noise at Start

Our results are best organized around the concept of Start as an autonomous submodule in the cell cycle. Variability in timing of Start, such as we observe in the *cln3 mbp1* background, is loosely analogous to extrinsic noise in Elowitz et al. (2002), Raser and O'Shea (2004), and Swain et al. (2002), in that it is upstream of all the events intrinsic to Start: once the program initiates, it proceeds robustly and with high internal coherence. In contrast, the high variability in level of *CLN2pr-GFP* expression that we observe in the *swi4* mutant constitutes loss of reliable intra-Start coherence: the response of one marker internal to Start relative to another is defective or mistimed. This kind of variability is loosely analogous to the decorrelation between two markers driven by identical promoters, "intrinsic" noise in Elowitz et al. (2002), Raser and O'Shea (2004), and Swain et al. (2002).

Interestingly, Swi4 and Cln3 were previously implicated in control of Start variability (MacKay et al., 2001); because only budding was assayed in that study, the distinction between extrinsic and intrinsic variability, or timing variability versus loss of intra-Start coherence, could not be made at that time.

Noise, Noise Suppression, and Evolution

We observe around 50% variability in wt cells for both cell size and timing of Start, consistent with earlier observations (Hartwell and Unger, 1977; Lord and Wheals, 1980, 1981, 1983). Other microorganisms (*E. coli* and fission yeast) (Stewart et al., 2005; Sveiczer et al., 2001) and embryos (Newport and Kirschner, 1984) display less variability. Even budding yeast, when growing in pseudo-hyphal mode (Kron et al., 1994), are much more synchronous in their cell cycles than the yeast-form cells we have analyzed. Thus, wild-type yeast (at least the

asymmetric yeast-form) has relatively noisy cell cycle control.

Such variability may be adaptive. Evolvability of gene expression noise was suggested based on analysis of *cis*- and *trans*-acting mutations altering extrinsic and intrinsic noise in various reporters (Raser and O'Shea, 2004). Among the benefits of variability could be a range of colony properties when confronted with a sudden change in environment; or variability could be a way of engaging natural homeostatic mechanisms or tuning sensory pathways (Xie and Seung, 2004). Nonadaptive causes of noise could be truly molecular (i.e., only a few molecules present for some crucial step) or could reflect extreme sensitivity to environment manifest at key transition points in the cell cycle such as bud formation and mitotic spindle assembly and integrity.

A surprising conclusion of our analysis is that the coherence of expression of the G1/S transcriptional program is demonstrably less than maximal in wt, as coherence is increased in the *cln3 mbp1 rme1* background relative to wt. Improved coherence appears to come at a cost, though, because the *cln3 mbp1 rme1* background simultaneously increases variability in inter-Start timing compared to wt. Thus the overall level of noise in wt may be an evolutionary compromise between requirements for both high-coherence and high-timing regularity.

Experimental Procedures

Yeast Strains

Standard methods were used throughout. The *CLN2pr-GFP* construct pSVA17 (Mateus and Avery, 2000) was integrated by *Eco*NI digestion and confirmed by Southern blotting analysis to be a single duplicative integration at *CLN2*. All strains were in the W303 background.

Time-Lapse Acquisition System

We created a time-lapse microscopy system derived from that used for studies of stochastic effects in prokaryotic transcriptional regulation (Elowitz et al., 2002; Rosenfeld et al., 2005). Fluorescent and phase-contrast images were acquired at 3 min resolution for 6 to 9 hr, without significant perturbation to growth rate of mother or daughter cells. Increased nuclear localization of Msn2, which has been shown to occur in response to stress from intense illumination (Jacquet et al., 2003), did not occur at the fluorescence exposure times used in our setup. A full characterization of the time-lapse setup is provided in the Supplemental Data.

Data Analysis

We created MATLAB software for automated image segmentation and fluorescence quantitation of yeast grown under time-lapse conditions and semiautomated assignment of microcolony pedigrees. Fluorescence intensity was determined automatically for the cell bodies identified by segmentation and analyzed by the program to identify *CLN2pr-GFP* peak amplitudes and the timing between *CLN2pr-GFP* peaks and bud emergence. For quantitation, we employed the total background-subtracted fluorescent signal divided by the cell body area as determined by the segmenter. We used this ratio as an approximation to the method used in standard RNA analysis, in which specific signal is divided by a nonspecific background level (e.g., control transcript). The alternative of using the total fluorescence per cell would only exaggerate the trends we document below, as the cell area and averaged fluorescence are nonnegatively correlated (data not shown). A full characterization of the data analysis is provided in the Supplemental Data.

Nuclear residence of Whi5-GFP and the presence of the Cdc10-GFP septin ring were scored by visual inspection of composite phase contrast-fluorescent movies and single-channel fluorescent movies, respectively. (See the Supplemental Data for a full description and some caveats related to scoring ambiguities; these ambiguities are unlikely to significantly affect our conclusions).

All MATLAB software is available upon request to E.D.S. (siggia@eds1.rockefeller.edu).

Supplemental Data

Supplemental Data include Supplemental Experimental Procedures, three figures, two tables, and Supplemental References and can be found with this article online at http://www.molecule.org/cgi/content/full/21/1/3/DC1/.

Acknowledgments

The authors would like to thank Michael Elowitz for invaluable help with establishing the time-lapse microscope setup, including the Visual Basic image acquisition software, as well as with initial time-lapse experiments. We also wish to thank Rob Sheridan and Ted Skolnick for their help in writing the MATLAB segmentation software and the MATLAB annotation GUI, respectively. We would like to thank Rahul Siddharthan for his assistance in creating the software used to generate yeast pedigrees. Finally, our thanks go to Kim Nasmyth, Richard Young, Kyung Lee, Mike Tyers, and Simon Avery for providing valuable strains and plasmids. This work was supported by the Howard Hughes Medical Institute (Predoctoral Fellowship to J.M.B.), the National Institutes of Health grant PHS GM047238 (to F.R.C.), the Burroughs Wellcome Fund (F.R.C. and E.D.S.), and the National Science Foundation grant DMR 0129848 (E.D.S.).

Received: July 12, 2005
Revised: September 22, 2005
Accepted: October 28, 2005
Published: January 5, 2006

References

Amon, A., Irniger, S., and Nasmyth, K. (1994). Closing the cell cycle circle in yeast: G2 cyclin proteolysis initiated at mitosis persists until the activation of G1 cyclins in the next cycle. Cell *77*, 1037–1050.

Bean, J.M., Siggia, E.D., and Cross, F.R. (2005). High functional overlap between MluI cell-cycle box binding factor and Swi4/6 cell-cycle box binding factor in the G1/S transcriptional program in *Saccharomyces cerevisiae*. Genetics *171*, 49–61.

Becskei, A., Kaufmann, B.B., and van Oudenaarden, A. (2005). Contributions of low molecule number and chromosomal positioning to stochastic gene expression. Nat. Genet. *37*, 937–944.

Cosma, M.P., Tanaka, T., and Nasmyth, K. (1999). Ordered recruitment of transcription and chromatin remodeling factors to a cell cycle- and developmentally regulated promoter. Cell *97*, 299–311.

Cosma, M.P., Panizza, S., and Nasmyth, K. (2001). Cdk1 triggers association of RNA polymerase to cell cycle promoters only after recruitment of the mediator by SBF. Mol. Cell *7*, 1213–1220.

Costanzo, M., Nishikawa, J.L., Tang, X., Millman, J.S., Schub, O., Breitkreuz, K., Dewar, D., Rupes, I., Andrews, B., and Tyers, M. (2004). CDK activity antagonizes Whi5, an inhibitor of G1/S transcription in yeast. Cell *117*, 899–913.

Cross, F.R. (1988). DAF1, a mutant gene affecting size control, pheromone arrest, and cell cycle kinetics of Saccharomyces cerevisiae. Mol. Cell. Biol. *8*, 4675–4684.

Cross, F.R. (1995). Starting the cell cycle: what's the point? Curr. Opin. Cell Biol. *7*, 790–797.

Cross, F.R. (2003). Two redundant oscillatory mechanisms in the yeast cell cycle. Dev. Cell *4*, 741–752.

Cross, F.R., and Tinkelenberg, A.H. (1991). A potential positive feedback loop controlling CLN1 and CLN2 gene expression at the start of the yeast cell cycle. Cell *65*, 875–883.

Cross, F.R., Hoek, M., McKinney, J.D., and Tinkelenberg, A.H. (1994). Role of Swi4 in cell cycle regulation of CLN2 expression. Mol. Cell. Biol. *14*, 4779–4787.

Cross, F.R., Schroeder, L., Kruse, M., and Chen, K.C. (2005). Quantitative characterization of a mitotic cyclin threshold regulating exit from mitosis. Mol. Biol. Cell *16*, 2129–2138.

de Bruin, R.A., McDonald, W.H., Kalashnikova, T.I., Yates, J., 3rd, and Wittenberg, C. (2004). Cln3 activates G1-specific transcription via phosphorylation of the SBF bound repressor Whi5. Cell *117*, 887–898.

Di Como, C.J., Chang, H., and Arndt, K.T. (1995). Activation of CLN1 and CLN2 G1 cyclin gene expression by BCK2. Mol. Cell. Biol. *15*, 1835–1846.

Dirick, L., and Nasmyth, K. (1991). Positive feedback in the activation of G1 cyclins in yeast. Nature *351*, 754–757.

Dirick, L., Bohm, T., and Nasmyth, K. (1995). Roles and regulation of Cln-Cdc28 kinases at the start of the cell cycle of Saccharomyces cerevisiae. EMBO J. *14*, 4803–4813.

Elowitz, M.B., Levine, A.J., Siggia, E.D., and Swain, P.S. (2002). Stochastic gene expression in a single cell. Science *297*, 1183–1186.

Epstein, C.B., and Cross, F.R. (1994). Genes that can bypass the CLN requirement for Saccharomyces cerevisiae cell cycle START. Mol. Cell. Biol. *14*, 2041–2047.

Hartwell, L.H., and Unger, M.W. (1977). Unequal division in Saccharomyces cerevisiae and its implications for the control of cell division. J. Cell Biol. *75*, 422–435.

Igual, J.C., Johnson, A.L., and Johnston, L.H. (1996). Coordinated regulation of gene expression by the cell cycle transcription factor Swi4 and the protein kinase C MAP kinase pathway for yeast cell integrity. EMBO J. *15*, 5001–5013.

Jacquet, M., Renault, G., Lallet, S., De Mey, J., and Goldbeter, A. (2003). Oscillatory nucleocytoplasmic shuttling of the general stress response transcriptional activators Msn2 and Msn4 in *Saccharomyces cerevisiae*. J. Cell Biol. *161*, 497–505.

Johnston, G.C., Pringle, J.R., and Hartwell, L.H. (1977). Coordination of growth with cell division in the yeast Saccharomyces cerevisiae. Exp. Cell Res. *105*, 79–98.

Jorgensen, P., and Tyers, M. (2004). How cells coordinate growth and division. Curr. Biol. *14*, R1014–R1027.

Jorgensen, P., Nishikawa, J.L., Breitkreutz, B.J., and Tyers, M. (2002). Systematic identification of pathways that couple cell growth and division in yeast. Science *297*, 395–400.

Kato, M., Hata, N., Banerjee, N., Futcher, B., and Zhang, M.Q. (2004). Identifying combinatorial regulation of transcription factors and binding motifs. Genome Biol. *5*, R56.

Koch, C., and Nasmyth, K. (1994). Cell cycle regulated transcription in yeast. Curr. Opin. Cell Biol. *6*, 451–459.

Koch, C., Moll, T., Neuberg, M., Ahorn, H., and Nasmyth, K. (1993). A role for the transcription factors Mbp1 and Swi4 in progression from G1 to S phase. Science *261*, 1551–1557.

Koch, C., Schleiffer, A., Ammerer, G., and Nasmyth, K. (1996). Switching transcription on and off during the yeast cell cycle: Cln/Cdc28 kinases activate bound transcription factor SBF (Swi4/Swi6) at start, whereas Clb/Cdc28 kinases displace it from the promoter in G2. Genes Dev. *10*, 129–141.

Kron, S.J., Styles, C.A., and Fink, G.R. (1994). Symmetric cell division in pseudohyphae of the yeast Saccharomyces cerevisiae. Mol. Biol. Cell *5*, 1003–1022.

Laabs, T.L., Markwardt, D.D., Slattery, M.G., Newcomb, L.L., Stillman, D.J., and Heideman, W. (2003). ACE2 is required for daughter cell-specific G1 delay in Saccharomyces cerevisiae. Proc. Natl. Acad. Sci. USA *100*, 10275–10280.

Lord, P.G., and Wheals, A.E. (1980). Asymmetrical division of Saccharomyces cerevisiae. J. Bacteriol. *142*, 808–818.

Lord, P.G., and Wheals, A.E. (1981). Variability in individual cell cycles of Saccharomyces cerevisiae. J. Cell Sci. *50*, 361–376.

Lord, P.G., and Wheals, A.E. (1983). Rate of cell cycle initiation of yeast cells when cell size is not a rate-determining factor. J. Cell Sci. *59*, 183–201.

MacKay, V.L., Mai, B., Waters, L., and Breeden, L.L. (2001). Early cell cycle box-mediated transcription of CLN3 and SWI4 contributes to the proper timing of the G(1)-to-S transition in budding yeast. Mol. Cell. Biol. *21*, 4140–4148.

Mateus, C., and Avery, S.V. (2000). Destabilized green fluorescent protein for monitoring dynamic changes in yeast gene expression with flow cytometry. Yeast *16*, 1313–1323.

Moffat, J., and Andrews, B. (2004). Late-G1 cyclin-CDK activity is essential for control of cell morphogenesis in budding yeast. Nat. Cell Biol. *6*, 59–66.

Nash, R., Tokiwa, G., Anand, S., Erickson, K., and Futcher, A.B. (1988). The WHI1+ gene of Saccharomyces cerevisiae tethers cell division to cell size and is a cyclin homolog. EMBO J. *7*, 4335–4346.

Nasmyth, K. (1996). At the heart of the budding yeast cell cycle. Trends Genet. *12*, 405–412.

Newport, J.W., and Kirschner, M.W. (1984). Regulation of the cell cycle during early Xenopus development. Cell *37*, 731–742.

Ozbudak, E.M., Thattai, M., Kurtser, I., Grossman, A.D., and van Oudenaarden, A. (2002). Regulation of noise in the expression of a single gene. Nat. Genet. *31*, 69–73.

Park, C.J., Song, S., Lee, P.R., Shou, W., Deshaies, R.J., and Lee, K.S. (2003). Loss of CDC5 function in Saccharomyces cerevisiae leads to defects in Swe1p regulation and Bfa1p/Bub2p-independent cytokinesis. Genetics *163*, 21–33.

Raser, J.M., and O'Shea, E.K. (2004). Control of stochasticity in eukaryotic gene expression. Science *304*, 1811–1814.

Rosenfeld, N., Young, J.W., Alon, U., Swain, P.S., and Elowitz, M.B. (2005). Gene regulation at the single-cell level. Science *307*, 1962–1965.

Schneider, B.L., Zhang, J., Markwardt, J., Tokiwa, G., Volpe, T., Honey, S., and Futcher, B. (2004). Growth rate and cell size modulate the synthesis of, and requirement for, G1-phase cyclins at start. Mol. Cell. Biol. *24*, 10802–10813.

Spellman, P.T., Sherlock, G., Zhang, M.Q., Iyer, V.R., Anders, K., Eisen, M.B., Brown, P.O., Botstein, D., and Futcher, B. (1998). Comprehensive identification of cell cycle-regulated genes of the yeast Saccharomyces cerevisiae by microarray hybridization. Mol. Biol. Cell *9*, 3273–3297.

Stewart, E.J., Madden, R., Paul, G., and Taddei, F. (2005). Aging and death in an organism that reproduces by morphologically symmetric division. PLoS Biol. *3*(*2*), e45 DOI: 10.1371/journal.pbio.0030045.

Stuart, D., and Wittenberg, C. (1994). Cell cycle-dependent transcription of CLN2 is conferred by multiple distinct cis-acting regulatory elements. Mol. Cell. Biol. *14*, 4788–4801.

Stuart, D., and Wittenberg, C. (1995). CLN3, not positive feedback, determines the timing of CLN2 transcription in cycling cells. Genes Dev. *9*, 2780–2794.

Sveiczer, A., Tyson, J.J., and Novak, B. (2001). A stochastic, molecular model of the fission yeast cell cycle: role of the nucleocytoplasmic ratio in cycle time regulation. Biophys. Chem. *92*, 1–15.

Swain, P.S., Elowitz, M.B., and Siggia, E.D. (2002). Intrinsic and extrinsic contributions to stochasticity in gene expression. Proc. Natl. Acad. Sci. USA *99*, 12795–12800.

Toone, W.M., Johnson, A.L., Banks, G.R., Toyn, J.H., Stuart, D., Wittenberg, C., and Johnston, L.H. (1995). Rme1, a negative regulator of meiosis, is also a positive activator of G1 cyclin gene expression. EMBO J. *14*, 5824–5832.

Tyers, M., Tokiwa, G., and Futcher, B. (1993). Comparison of the Saccharomyces cerevisiae G1 cyclins: Cln3 may be an upstream activator of Cln1, Cln2 and other cyclins. EMBO J. *12*, 1955–1968.

Wijnen, H., Landman, A., and Futcher, B. (2002). The G(1) cyclin Cln3 promotes cell cycle entry via the transcription factor Swi6. Mol. Cell. Biol. *22*, 4402–4418.

Xie, X., and Seung, H.S. (2004). Learning in neural networks by reinforcement of irregular spiking. Phys. Rev. E Stat. Nonlin. Soft Matter Phys. *69*, 041909.